Stochastic Resonance Between Counterpropagating Walls in a Neighborhood of a Nonequilibrium Ising-Bloch Bifurcation

Matias G. dell'Erba, Gonzalo G. Izús, Roberto R. Deza and Horacio S. Wio[1]
[1]*IFIMAR, UNMDP, IFCA*
(Dated: December 5, 2009)

We investigate ...

PACS numbers:

I. INTRODUCTION

Nonequilibrium Ising-Bloch (NIB) transitions have been identified as an important mechanisms of pattern formation in reaction-diffusion [1–5], optical [6–8] and liquid crystal systems [8–10]. It consists in a pitchfork bifurcation where a stationary (Ising) front loses stability to a pair of counter-propagating (Bloch) fronts. In a NIB transition, the destabilization of an Ising front is initiated by a -critical- eigenvector which coincide with the translational (Goldstone) mode at the critical point [11]. The coexistence of two Bloch fronts far beyond the bifurcation allows the formation of patterns such as traveling domains and rotating spiral waves in two spatial dimension. This bifurcation is closely related to chiral symmetry breaking in magnetic domain walls [12] and forced oscillatory systems [3]. The bifurcated fronts may may produce complex spatiotemporal phenomena in 2D involving spontaneous nucleation of spiral waves followed by domain breakup [13–16].

Activator-inhibitor systems with nondiffusing inhibitors, like the FitzHugh Nagumo model, provide a good example. In these systems, a diffusing autocatalytic species (activator) produce a second substance (inhibitor) in another time scale, which in turn consumes the activator, thus introducing a negative feedback. For fast inhibitors, in the bistable regime, the dynamics exhibits Ising domain walls and eventually converge to an uniform state in two spatial dimension. For sufficiently slow kinetics –in fact for the activator-inhibitor time scales ratio ϵ below a critical threshold ϵ_c– (i.e, beyond the NIB bifurcation) Bloch domain walls are the stable interface and traveling pulses, periodic wave trains and spiral waves appear. Structurally, these Bloch walls (BW) differ from an Ising wall (IW) in that the inhibitor step-like profile is displaced with respect of the activator one at the core of the wall. The magnitude and the sign of the displacement determine the speed and direction of propagation, respectively. The velocity c of the bifurcated fronts (asymptotically) follows a square-root law: $c \propto \sqrt{\epsilon_c - \epsilon}$ [5].

In this paper we want to explore the possibility to observe SR between Bloch domain walls. In particular, to characterize the scale-law of the SNR with the distance to the critical point in terms of an effective nonequilibrium potential (NEP). The paper is organized as follows: in Section II we introduce the model, the fronts solutions (Ising and Bloch wall) and the external forcings (subthreshold signal and noise). In Section III we introduce the order parameter and we discuss the stochastic resonance of the chirality in terms of the relevant parameters. The conclusion are presented in Section IV.

II. THE FITZHUGH-NAGUMO MODEL

A. The equations

We consider here a dimensionless nongradient activator-inhibitor reaction-diffusion model of the FitzHugh Nagumo type [17, 18], which is a canonical model for activator-inhibitor systems and exhibits a NIB bifurcation [1]

$$\begin{aligned} \frac{\partial u}{\partial t} &= \nabla^2 u + u - u^3 - v \\ \frac{\partial v}{\partial t} &= \epsilon\,(u - a\,v) \end{aligned} \tag{1}$$

In the context of chemical reactions u and v represents normalized concentrations of key chemical species. Two-variable models like (1) are obtained in this context by adiabatic elimination of fast reacting species, and in this process transport terms and concentrations are normalized. We choose a such that Eqs.(**??**) describe a bistable medium being the two linearly stable stationary solutions: (u_+, v_+) (up state) and (u_-, v_-) (down state), where $u_+ = -u_- = \sqrt{1 - a^{-1}}$ and $v_+ = -v_- = u_+/a$. Note that the up and down states have the parity symmetry $(u_-, v_-) = -(u_+, v_+)$ and the system is invariant under the change $(u, v) \to (-u, -v)$.

B. The fronts

Eqs.(1) have for all $\epsilon > 0$ a stationary (Ising) front solution [5]

$$u_0(x) = -u_+ \tanh(u_+ x/\sqrt{2}),\ v_0(x) = a^{-1} u_0(x) \tag{2}$$

which connects the up state at $x = -\infty$ with the down one at $x = +\infty$ (see Fig.1). Note that the wall vanishes at the core, and due to the parity symmetry the front: $(u_0(-x), v_0(-x))$ is also a stationary solution.

For $\epsilon < \epsilon_c = a^{-2}$ two additional (Bloch) front solutions appear, propagating at velocities

$$c = \pm \left[\frac{5}{2u_+^2} (\epsilon_c - \epsilon) \right]^{1/2} \quad (3)$$

The leading-order forms for these fronts for $|c| << 1$ are [5]

$$u(x,t) = u_0(x - ct),\ v(x,t) = a^{-1}\, u_0(x - ct + ca) \quad (4)$$

where the v-front is translated with respect to the u field by an amount proportional to c (see Figs.2). An useful distinction between Ising and Bloch fronts can be made by defining a "phase" $\phi(x) = \tan^{-1}(v(x)/u(x))$ and a "norm" $\rho(x) = \sqrt{u(x)^2 + v(x)^2}$. Across an Ising front the phase is constant except at the core of the wall where it jumps in π and the norm vanishes. In a Bloch front the phase rotates by an angle π smoothly and the norm never vanishes.

C. The external forcing

As results from Fig.2, transitions between Bloch walls with opposite chirality are associated to changes in the core of the wall, being the Ising core the barrier which the system must "bypass" to go from one Bloch wall to the other one.

In order to explore SR between the two equivalent dynamical attractors, we first include in the time-evolution equation a noise source $\xi(x,t)$ and, finally, we assume that the system is adiabatically forced by a slow external periodic signal $S(t)$, yielding to a stochastic partial differential equation for the random fields:

$$\begin{aligned} \frac{\partial u}{\partial t} &= \nabla^2 u + (u + S(t)) - u^3 - v + \xi(x,t) \\ \frac{\partial v}{\partial t} &= \epsilon\,[u - a\,v] \end{aligned} \quad (5)$$

where we make the simplest assumptions about the fluctuation term $\xi(x,t)$, i.e., it is an additive Gaussian white noise with noise strength γ, zero mean and delta-correlated in space and time:

$$\begin{aligned} < \xi(x,t) > &= 0 \\ < \xi(x,t)\,\xi(x',t') > &= 2\gamma\,\delta(t-t')\,\delta(x-x'). \end{aligned} \quad (6)$$

In Figs.3 we show the effects produced by the external forcing $S(t) = \delta\,\cos(\omega_0 t)$ in terms of the nullclines of the system. The value of δ was selected in order to obtain an appreciable figure. Note that the forcing produces a global change in the relative stability of the uniform solutions.

III. STOCHASTIC RESONANCE

A. Order parameter

Numerical simulations of Eqs.(5) without external signal ($S = 0$) show that noise-induced jumps between traveling BWs of opposite chirality are possible. This fact open the possibility to have SR. i.e., an enhancement of the output signal-to-noise ratio (SNR) caused by injection of an optimal amount of noise.

For a better characterization of the resonance we first introduce the "chirality field": $\eta(x,t) = u(x,t) - a\,v(x,t)$ which essentially measures deviation from stationarity, i.e., it is zero, positive or negative for IW, or BW's cores with positive or negative chirality, respectively. Jumps between dynamical attractors basically takes place at the core of the wall, therefore we introduce a reduced order parameter $\eta_R(t)$ to capture the resonant dynamics:

$$\eta_R(t) = \int_{core} [u(x,t) - a\,v(x,t)]\,dx \quad (7)$$

which allow us to discriminate between BWs of opposite chirality and also IWs in a direct way. Note that $\eta_R \sim 0$ corresponds to IW while the sign of η_R determines the chirality of the BWs.

B. Partial synchronization

A partial synchronization of chirality with the external signal is numerically observed for selected values of the noise intensity, as we show in fig.4 for a typical realization of Eqs.(5). Note that positive chirality corresponds to right motion, while negative values of η_R are associated with left motion of the wall, respectively. To illustrate this point, in fig.5 we show the corresponding core position x_c as a function of time. Reflection at the boundaries (at $x = \pm 204$) take place due to Neumann boundary conditions. Transition from left (right) motion to right (left) motion takes place basically with the signal at $+\delta$ $(-\delta)$, by reflecting the symmetric bistability. As expected, a maximum at $\omega = \omega_0$ is observed for the absolute value of the spectral density $S_D(\omega)$, as we illustrate in fig.6 for a characteristic realization of Eqs.(5).

C. Stochastic Resonance

We numerically observe that $|S_D(\omega)|$ depend on γ in a non-monotonic way. After normalize by the background spectrum at ω_0, the SNR exhibits a typical stochastic resonance's behavior for a bistable system. We illustrate this point in fig 7 for several external frequencies in the adiabatic regime. Note that the SR takes place between dynamical attractors that "carry with them" the saddle barrier.

Although a nonequilibrium potential is not known for $\epsilon < \epsilon_c$, it can be expected that it must share the main properties of the canonical NEP for the normal form of a pitchfork bifurcation. In consequence, some expression like

$$\frac{d\eta_r}{dt} = (\epsilon_c - \epsilon)\,\eta_R - \eta_R^3 \tag{8}$$

can be expected for a scaled order parameter. Transitions between both attractors are then ruled-out by NEPs like [22]

$$\Phi = -(\epsilon - \epsilon_c)\,\eta_R^2 + \frac{\eta_R^4}{4}. \tag{9}$$

In particular, a linear dependence with $(\epsilon_c - \epsilon)^2$ is expected to be for the NEP's difference between the saddle point (i.e, the IW) and the equivalent local attractors (i.e, the BWs), at least in a neighborhood of the NIB bifurcation. This fact originates a linear dependence of $\log(SNR)$ with $(\epsilon_c - \epsilon)^2$, as we illustrate in fig.8 for characteristic realizations of Eqs.(5). We remark that this fact was numerically confirmed in the neighborhood of the NIB transition for 1D systems while some deviation can be expected in 2D systems due to the presence of defects.

IV. CONCLUSION

We have investigated the stochastic resonance between dynamical attractors in a neighborhood of as non-equilibrium Ising-Bloch bifurcation. In particular, we have showed that the cooperative effect between noise and small-amplitude signal can originates an enhancement of the rate of transitions between the counter-propagating Bloch walls, as illustrates the spectral properties of an effective order parameter. Finally, we have introduced an qualitative non-equilibrium potential that describes the pitchfork bifurcation. From its analysis, a scale-law for the SNR was theoretically predicted and numerically confirmed.

V. ACKNOWLEDGEMENTS

... We...

[1] J. Rinzel and D. Terman, SIAM J. Appl. Math. **42**, 1111 (1980).
[2] H.Ikeda, M. Minura, and Y. Nishiura, Nonl. Anal. TMA **13**, 507 (1989).
[3] P. Coullet, J. Lega, B. Houchmanzadeh and J. Lajzerowicz, Phys. Rev. Lett **65**, 1532 (1990).
[4] M. Bode, A. Reuter, R. Schmeling, and H. Purwins, Phys. Lett. A **185**, 1532 (1990)
[5] A. Hagberg, and E. Meron, Nonlinearity
[6] G. Izús, M. Santagiustina and M. San Miguel, Opt. Lett. B **19**, 1454 (2000).
[7] G. Izús, M. Santagiustina and M. San Miguel, Phys. Rev. E **64**, 056231 (2001).
[8] C. Elphick, A. Hagberg, B. A. Malomed, E. Meron, Phys. Lett. A **230**, 33-37 (1997).
[9] T. Frisch, S. Rica, P. Coullet and J. Gilli, Phys. Rev. Lett. **72**, 1471 (1994).
[10] N. Nasuno, N. Yoshimo, and S. Kai, Phys. Rev. E **51**, 1598 (1995).
[11] Phys. Rev. E ...(2001)
[12] J. Lajzerowicz and J. Niez, J. Physique Lett. **40**, 165 (1979).
[13] A. Hagberg, and E. Meron, Phys. Rev. Lett.**72**, 2494 (1994)
[14] A. Hagberg, and E. Meron, Chaos **4**, 477 (1994)
[15] C. Elphick, A. Hagberg, and E. Meron, Phys. Rev. E **51**, 3052 (1995).
[16] A. Hagberg, and E. Meron, Phys. Rev. Lett **78**, 1166 (1997).
[17] R. Fitzhugh, Biophys. J. **1**, 445 (1961).
[18] J. Nagumo, S. Arimoto and S. Yoshizawa, Proc. IREE Aust. **50**, 2061 (1962),
[19] G. Nicolis and I. Prigogine, *Self-Organization in Non-equilibrium Systems* (Wiley, New York, 1977).
[20] H.S. Wio, *An Introduction to Stochastic Processes and Nonequilibrium Statistical Physics* (World Scientific, 1994).
[21] M.C. Cross and P.C. Hohenberg, Rev. Mod. Phys. **65**, 851 (1993).
[22] R. Graham and T. Tél, Phys. Rev A **35**, 1328 (1987).

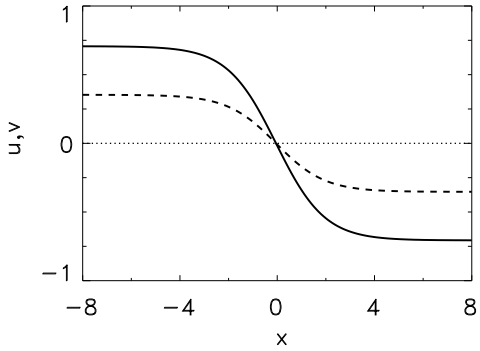

FIG. 1: Plot of an Ising domain wall. Solid (dashed) line: u (v). Note that the wall vanishes at the core and $u_0(x) = a * u_0(x)$ along the wall. Parameters are: $a = 2$ and $\epsilon = 0.5$. The zero level is indicated in dotted line as reference.

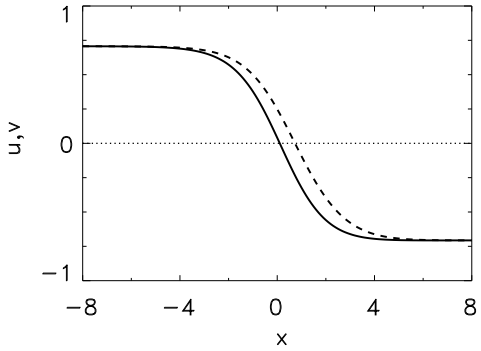

Fig. 2a

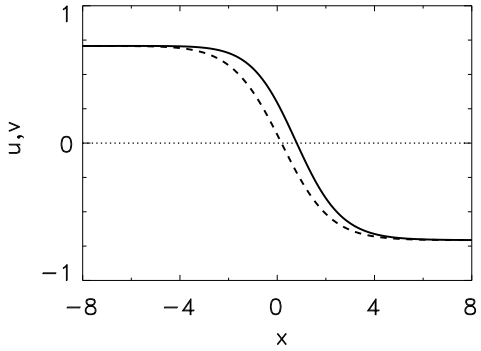

Fig. 2b

FIG. 2: Bloch domain walls. Solid (dashed) line: u ($a * v$). Note that the walls do not vanish at the core. Parameters are: $a = 2$ and $\epsilon = 0.23$. The zero level is indicated in dotted line as reference. A) Positive chirality, B) Negative chirality. The BWs connect the same asymptotic states, but they move in opposite sense, with the inhibitor front following the activator one.

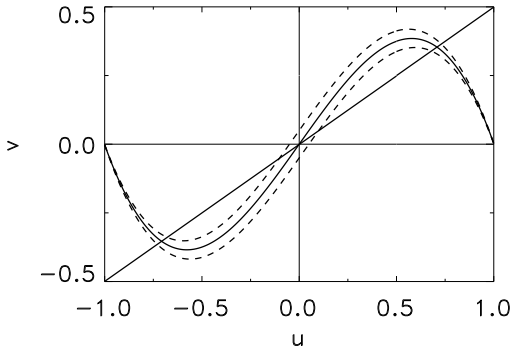

FIG. 3: Nullclines of Eqs.(1) under external additive forcing. With full line we indicate the no signal case. In dotted lines we indicate the cases where the signal amplitude is maximum and minimum, respectively. The amplitude δ of the external signal was magnified in a factor 50 to have an appreciable picture.

Fig. 3

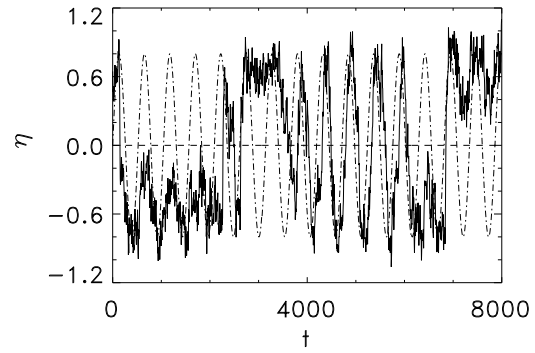

FIG. 4: Chirality as a function of time. The (scaled) external signal is also showed in dotted line as reference. Some jumps in chirality are induced by reflection of the core at the system's boundaries (see fig. 5). Paremeters are $a = 2$, $\delta = 0.001$ and ...

Fig. 4

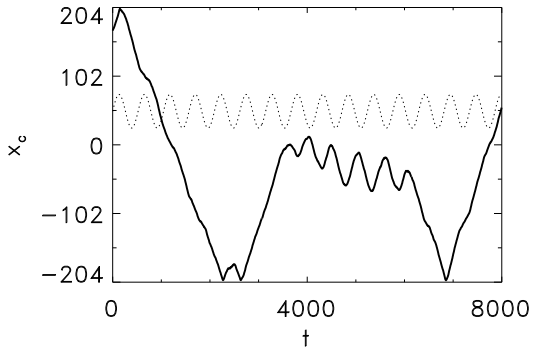

FIG. 5: Core position x_c as a function of time. Neumann boundary conditions induce reflections of the wall's motion at the boundaries. The others chirality jumps are induced by noise under the effect of the external signal. Parameters are the same of the previous figure

Fig. 5

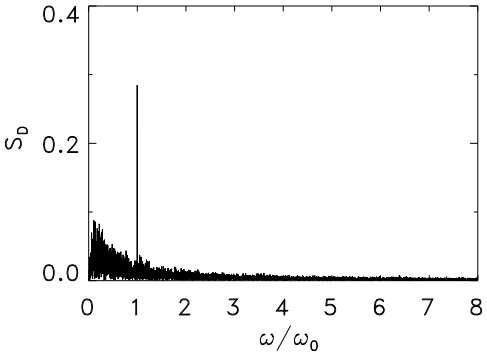

FIG. 6: Absolute value of the spectral density S_D as a function of the scaled frequency ω/ω_0 (ω_0 the signal frequency). Parameters are the same of the previous figure

Fig. 6

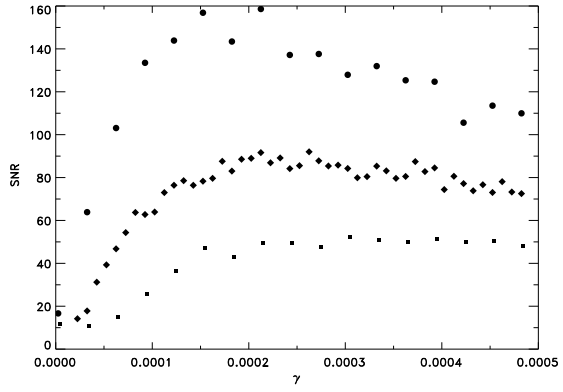

FIG. 7: SNR as a function of γ for selected values of the external frequency ω_0). Here $a = 2$, $\delta = 0.001$ and ...

Fig. 6

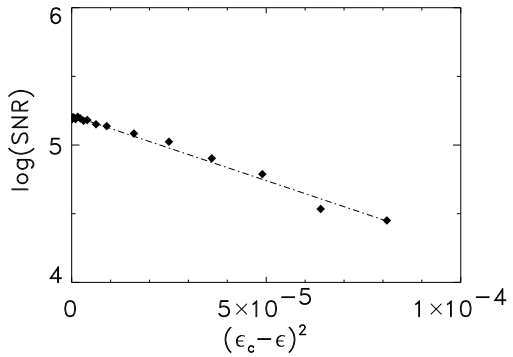

FIG. 8: $\ln(SNR)$ vs. $(\epsilon_c-\epsilon)^2$ in the neighborhood of the non-equilibrium Ising-Bloch bifurcation. Here $a = 2$, $\delta = 0.001$, $\gamma = 0.00018$ and $\omega_0 = 0.012$

Fig. 7